

# Cyanopolyynes as a probe of infall in Serpens South

Rachel Friesen (Dunlap Institute)

L. Medeiros<sup>1,2</sup>, S. Schnee<sup>2</sup>, T. L. Bourke<sup>3</sup>, J. Di Francesco<sup>4,5</sup>,

R. Gutermuth<sup>6</sup>, P. C. Myers<sup>3</sup>



<sup>1</sup> University of California - Berkeley <sup>2</sup> NRAO <sup>3</sup> Harvard-Smithsonian CfA <sup>4</sup> NRC-Herzberg <sup>5</sup> University of Victoria <sup>6</sup> University of Massachusetts - Amherst

**Abstract:** Cyanopolyynes are carbon-chain molecules of the form  $\text{HC}_{2n+1}\text{N}$ . At higher  $n$ , these molecules are among the longest and heaviest molecules found in the interstellar medium, and to date have been primarily seen toward several nearby, low-mass star forming regions, and in the atmospheres of AGB stars. We have detected bright  $\text{HC}_7\text{N}$   $J = 21-20$  emission toward multiple locations in the Serpens South cluster-forming region using the K-Band Focal Plane Array at the Robert C. Byrd Green Bank Telescope.  $\text{HC}_7\text{N}$  is seen primarily toward cold filamentary structures that have yet to form stars, largely avoiding the dense gas associated with small protostellar groups and the main central cluster of Serpens South.

Toward some  $\text{HC}_7\text{N}$  'clumps', we find consistent variations in the line centroids relative to  $\text{NH}_3$  (1,1) emission, as well as systematic increases in the  $\text{HC}_7\text{N}$  non-thermal line widths, which we argue reveal infall motions onto dense filaments within Serpens South with mass accretion rates of  $\dot{M} \sim 2 - 5 M_\odot \text{ Myr}^{-1}$ . This result extends the known star-forming regions containing significant  $\text{HC}_7\text{N}$  emission from typically quiescent regions, like the Taurus molecular cloud, to more complex, active environments.

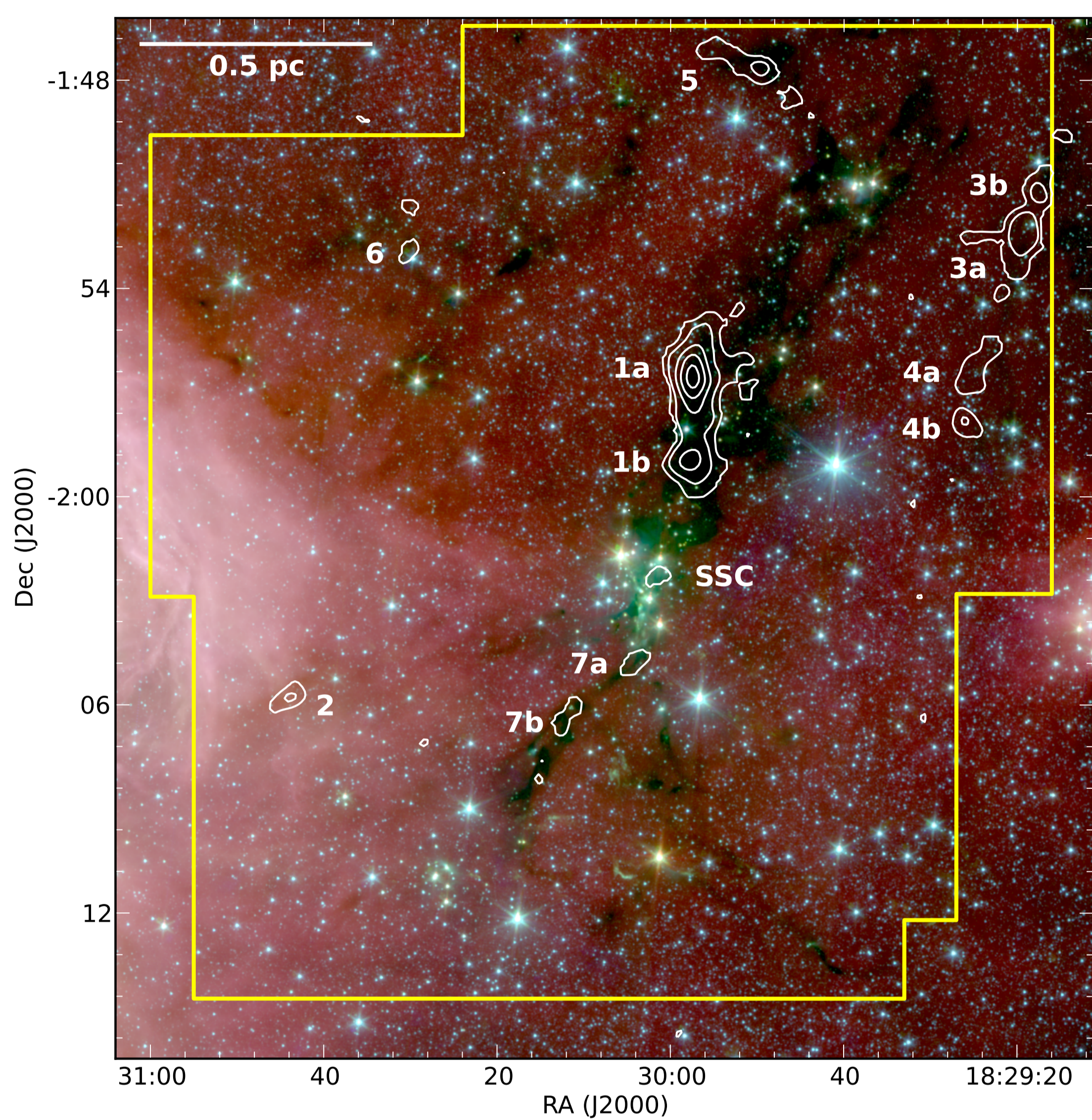


**Figure 1 (left):** Spitzer RGB (8  $\mu\text{m}$ , 4.5  $\mu\text{m}$ , 3.6  $\mu\text{m}$ ) image of the Serpens South protocluster (Gutermuth et al. 2008). White contours show integrated  $\text{HC}_7\text{N}$   $J = 21-20$  emission at 0.15  $\text{K km s}^{-1}$  ( $4\sigma$ ), 0.3  $\text{K km s}^{-1}$ , 0.6  $\text{K km s}^{-1}$ , 0.9  $\text{K km s}^{-1}$ , and 1.2  $\text{K km s}^{-1}$ . Individual  $\text{HC}_7\text{N}$  emission peaks are labeled. The physical scale assumes  $d = 260 \text{ pc}$ . Yellow contours show the map extent where the rms noise per velocity channel of width 0.15  $\text{K km s}^{-1}$  is  $\sigma < 0.1 \text{ K}$ .

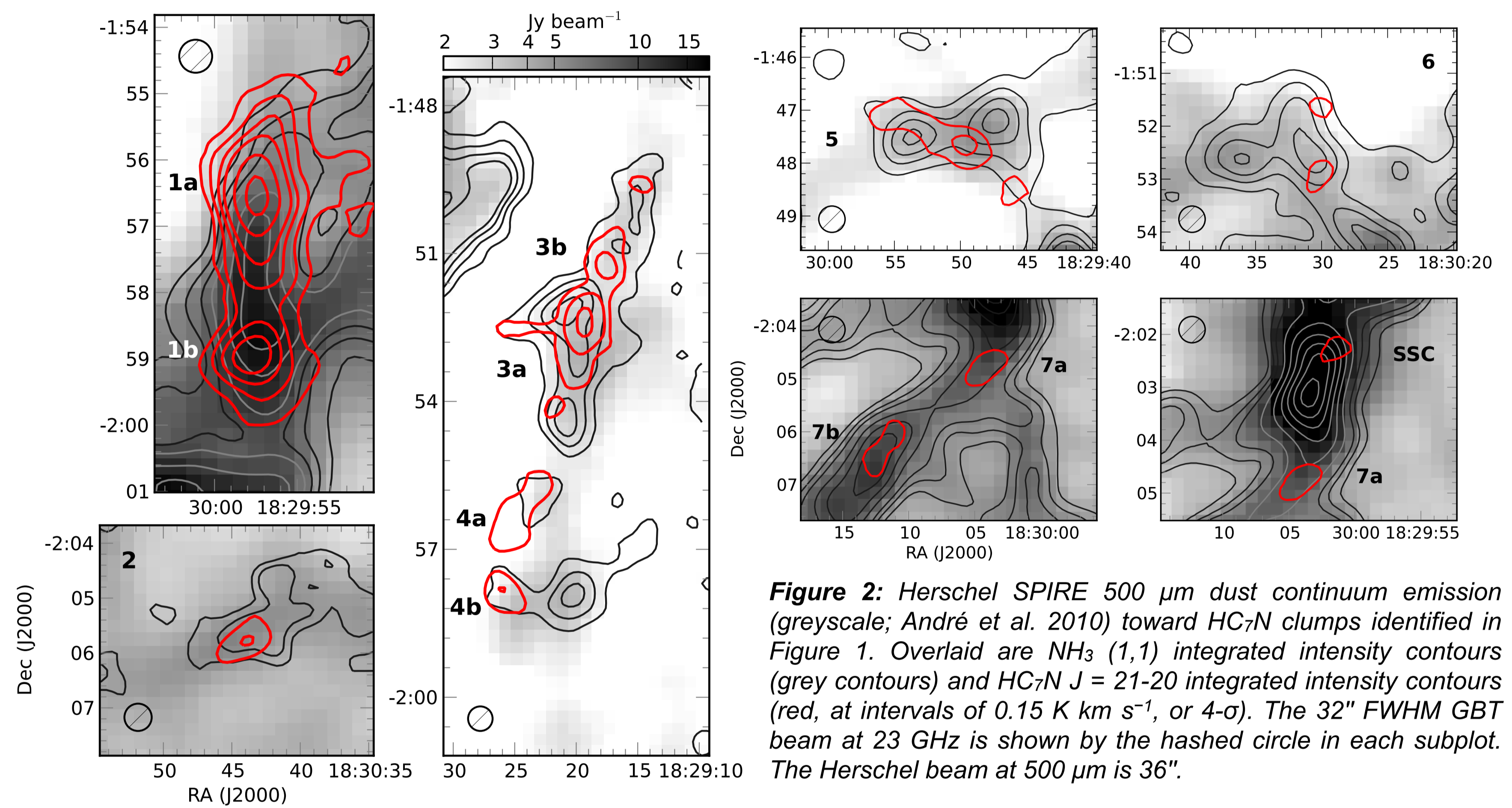


**Figure 2:** Herschel SPIRE 500  $\mu\text{m}$  dust continuum emission (greyscale; André et al. 2010) toward  $\text{HC}_7\text{N}$  clumps identified in Figure 1. Overlaid are  $\text{NH}_3$  (1,1) integrated intensity contours (grey contours) and  $\text{HC}_7\text{N}$   $J = 21-20$  integrated intensity contours (red, at intervals of 0.15  $\text{K km s}^{-1}$ , or  $4\sigma$ ). The 32" FWHM GBT beam at 23 GHz is shown by the hashed circle in each subplot. The Herschel beam at 500  $\mu\text{m}$  is 36".

**Chemistry:**  $\text{HC}_7\text{N}$  emission peaks are rarely co-located with those of either  $\text{NH}_3$  or continuum, although the required line excitation conditions are similar. The distribution of  $\text{HC}_7\text{N}$  and  $\text{NH}_3$  can be explained through simple chemical models of cold, dense gas:  $\text{NH}_3$  has a long formation timescale at a given gas density. Long carbon-chain molecules like  $\text{HC}_7\text{N}$  are produced rapidly in cold, dark clouds, but high abundances are only found well before the models reach a steady-state chemical equilibrium (Herbst & Leung 1989). The relative abundance of  $\text{NH}_3$  to  $\text{HC}_7\text{N}$  suggests that the  $\text{HC}_7\text{N}$  is tracing gas that has been at densities  $n \sim 10^4 \text{ cm}^{-3}$  for timescales  $t \sim 1 - 2 \times 10^5 \text{ yr}$  (Fig. 3).

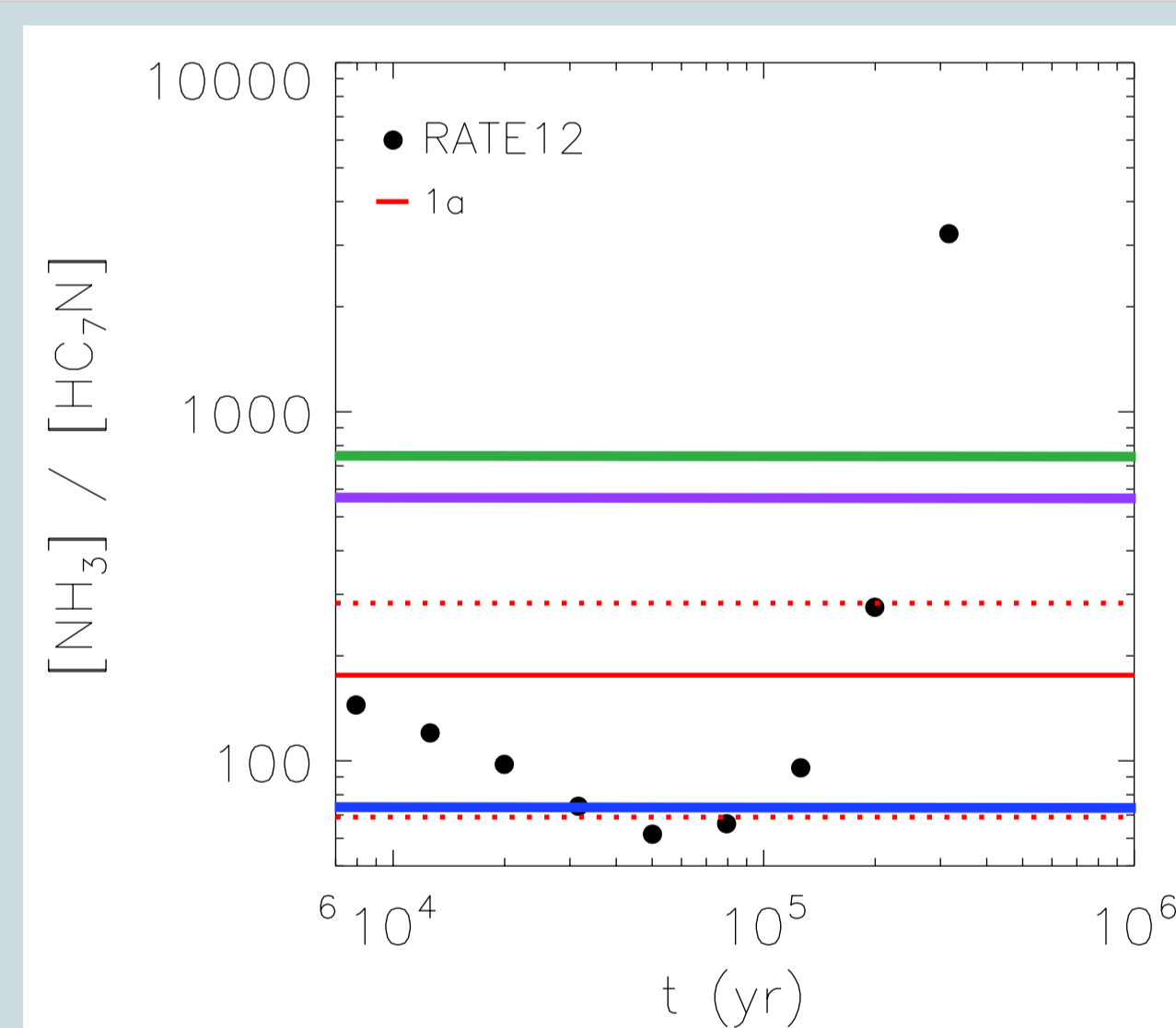


**Figure 3:** Black points show predictions from the 'dark cloud' chemical model ( $n = 10^4 \text{ cm}^{-3}$ ,  $T = 10 \text{ K}$ ,  $A_v = 10$ ) by McElroy et al. (2013) for the  $[\text{NH}_3]/[\text{HC}_7\text{N}]$  ratio as a function of time. Red lines show the mean value (solid) and standard deviation (dashed) for  $\text{HC}_7\text{N}$  clump 1a. Clumps 2, 3a, 3b, 4a, and 4b have mean abundance ratios  $\sim 70$  (blue), while the SSC and 7b show  $[\text{NH}_3]/[\text{HC}_7\text{N}] \sim 500 - 700$  (purple & green lines).

## Is $\text{HC}_7\text{N}$ tracing infalling material?

Toward the  $\text{HC}_7\text{N}$  clumps 1a and 1b, we find:

- supercritical  $M/L$  relative to equilibrium, isothermal cylinder
- plane-of-the-sky velocity gradients, pointing to increased  $[\text{HC}_7\text{N}]/[\text{NH}_3]$  abundance ratios (Fig. 4a,b)
- coherent variations in  $v_{\text{LSR}}$  between  $\text{HC}_7\text{N}$  and  $\text{NH}_3$  consistent in direction with infall onto a filament (Fig. 4c)
- increased non-thermal line widths relative to  $\text{NH}_3$  emission by  $\sim 0.07 \text{ km s}^{-1}$  (Fig. 4d)

Mass accretion rate along filament (from velocity gradients and line widths)  $\sim 14 M_\odot \text{ Myr}^{-1}$ , comparable to the filament mass of  $\sim 30 M_\odot$ .

Toward the other  $\text{HC}_7\text{N}$  clumps, we find similar variations in  $v_{\text{LSR}}$  between  $\text{HC}_7\text{N}$  and  $\text{NH}_3$ , as well as smooth velocity gradients in the  $\text{HC}_7\text{N}$  emission.

## Correlation between velocity and abundance gradients

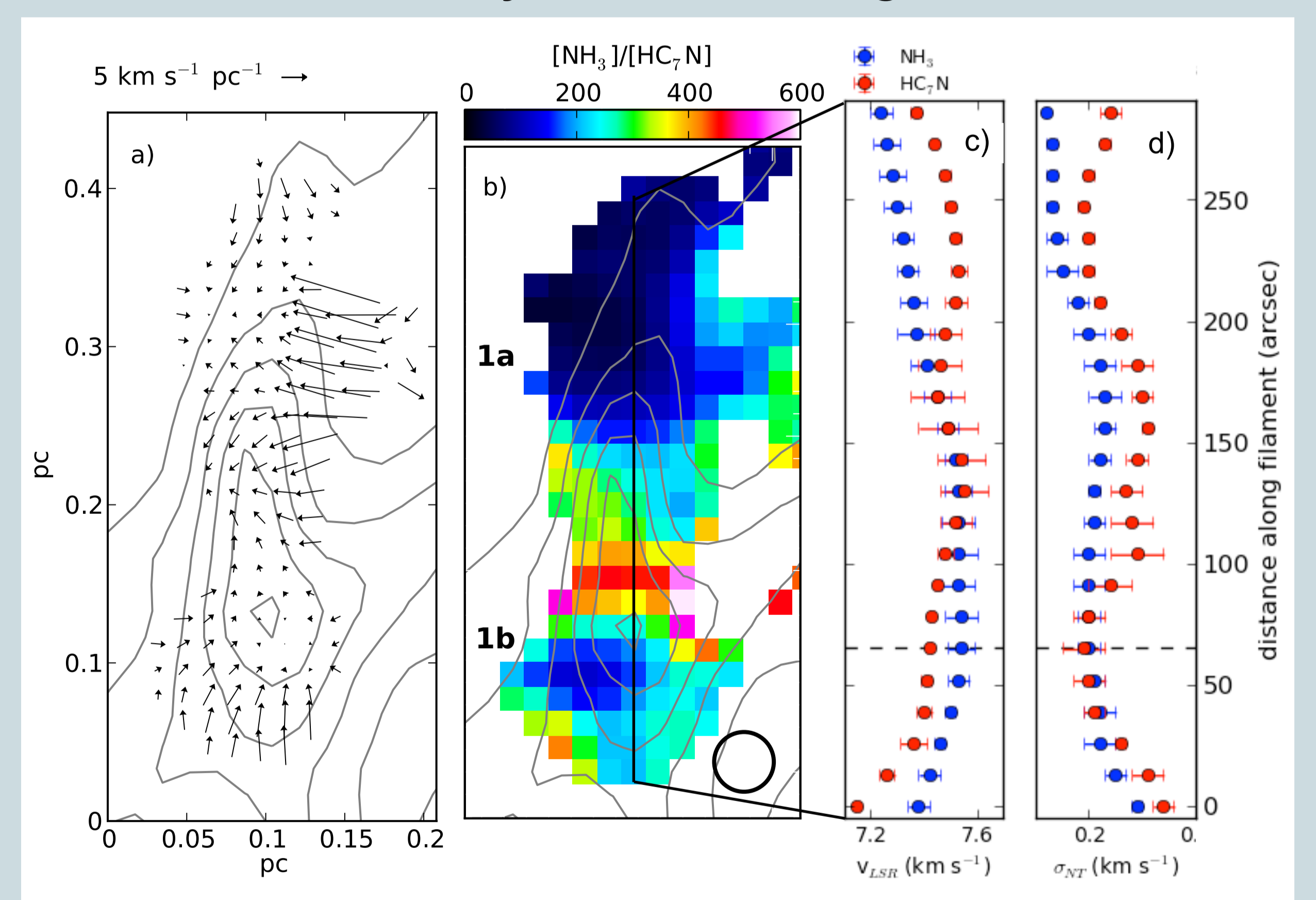


**Figure 4:** a) Gradient in line-of-sight velocity ( $v_{\text{LSR}}$ ) of  $\text{HC}_7\text{N}$  emission toward  $\text{HC}_7\text{N}$  clumps 1a and 1b. In both figures, grey contours show the 1.1 mm continuum emission. b) Map of the  $[\text{NH}_3]/[\text{HC}_7\text{N}]$  abundance ratio toward the same region. The circle shows the 32" FWHM beam. c)  $v_{\text{LSR}}$  derived from fits of  $\text{NH}_3$  (blue symbols) and  $\text{HC}_7\text{N}$  (red symbols) averaged in increments of 13" in declination along a line of constant R.A. that follows the filament axis (shown in black). Error bars show the  $1-\sigma$  spread in values along the perpendicular (R.A.) axis. d) The non-thermal line width,  $\sigma_{\text{NT}}$ , for  $\text{NH}_3$  (blue symbols) and  $\text{HC}_7\text{N}$  (red symbols) along the filamentary axis.

The simultaneous mapping of  $\text{HC}_7\text{N}$  with  $\text{NH}_3$  has allowed us to detect  $\text{HC}_7\text{N}$  at low abundances in regions where it otherwise may not have been looked for.  $\text{HC}_7\text{N}$  reveals newly dense material in the cluster, either through recent accretion onto existing dense cores or newly-formed cores, and facilitates further analysis of how filaments form and accumulate mass. Serpens South is also an ideal target to study long carbon chain and molecular ion chemistry.

## References:

- André et al. 2010, A&A 518, 102 • Friesen et al. 2013, MNRAS, submitted • Gutermuth et al. 2008, ApJ, 673, 151 • Herbst & Leung. 1989, ApJS, 69, 271 • McElroy et al. 2013, A&A, 550, 36